

1 **Effective biomass fractionation and lignin stabilization using a diol DES system**

2 Jinyuan Cheng<sup>a</sup>, Chen Huang<sup>a,b,c,\*</sup>, Yunni Zhan<sup>a</sup>, Shanming Han<sup>a</sup>, Jia Wang<sup>b</sup>, Xianzhi

3 Meng<sup>c</sup>, Chang Geun Yoo<sup>f</sup>, Guigan Fang<sup>a,b,\*</sup>, Arthur J. Ragauskas<sup>c,d,e</sup>

4 <sup>a</sup>Institute of Chemical Industry of Forest Products, Chinese Academy of Forestry,

5 Jiangsu Province Key Laboratory of Biomass Energy and Materials, Nanjing 210042,

6 China.

7 <sup>b</sup>Co-Innovation Center for Efficient Processing and Utilization of Forest Resources,

8 Nanjing Forestry University, Nanjing 210037, China.

9 <sup>c</sup>Department of Chemical and Biomolecular Engineering, University of Tennessee

10 Knoxville, Knoxville, TN 37996, USA.

11 <sup>d</sup>Department of Forestry, Wildlife, and Fisheries, Center for Renewable Carbon, The

12 University of Tennessee Institute of Agriculture, Knoxville, TN 37996, USA.

13 <sup>e</sup>Joint Institute for Biological Science, Biosciences Division, Oak Ridge National

14 Laboratory, Oak Ridge, TN 37831, USA.

15 <sup>f</sup>Department of Chemical Engineering State University of New York College of

16 Environment Science and Forestry, Syracuse, New York 13210-2781, United States.

17

18 **Abstract**

19 A sustainable and renewable biorefinery will increase the economic viability of

20 lignocellulose-derived products. In this study, a diol-based deep eutectic solvent (DES)

21 was developed to reduce the recalcitrance of bamboo, facilitate saccharification and

22 valorize the lignin fraction. The DES pretreatment dramatically enhanced glucan

23 digestibility by the effective removal of lignin (as high as 85.45%) and xylan (91.12%).

24 Notably, the recovered lignin from DES pretreatment was protected during the

25 fractionation, showing well-preserved  $\beta$ -O-4 structures (31.82%-59.06%). The

26 mechanism of lignin protection was analyzed to be accomplished by incorporating the  
27 diol hydroxyl functional groups into the  $\alpha$  position of the lignin  $\beta$ -O-4 structure *via*  
28 etherification. This study highlighted that diol DES is a promising pretreatment solvent  
29 to valorize both cellulose and lignin fractions with high enzymatic hydrolysis yield and  
30 high-quality lignin co-product.

31 **Keywords:** diol DES, delignification, lignin protection, lignin valorization

32 **1. Introduction**

33 The depletion of fossil fuels and the consequent environmental issue have  
34 forced society to seek renewable, sustainable, and eco-friendly alternatives [1].  
35 Lignocellulosic biomass is the most abundant renewable resource on earth and  
36 has been deemed as an ideal alternative to petroleum [2]. Lignocellulosic  
37 biomass is composed primarily of cellulose, hemicellulose, and lignin [3], in  
38 which cellulose and hemicellulose are mainly comprised of sugars that can be  
39 depolymerized and further converted into chemicals and fuels. As to lignin, it is  
40 constituted of guaiacyl (G), syringyl (S), and/or *p*-hydroxyphenyl (H) units,  
41 which are bonded through a variety of C-O (*e.g.*,  $\alpha$ -O-4,  $\beta$ -O-4 and 4-O-5) and  
42 C-C (*e.g.*,  $\beta$ -5,  $\beta$ - $\beta$ , 5-5, and  $\beta$ -1) linkages [4]. As widely acknowledged that  
43 lignin and hemicellulose are covalently crosslinked with each other and interact  
44 with cellulose *via* hydrogen bonds and van der Waal forces, resulting in the  
45 natural recalcitrance of biomass [5]. Therefore, pretreatment has been  
46 investigated as a pivotal processing step for the effective biomass conversion [6].

47 In a conventional biorefinery or pulping processes, lignin is often treated as  
48 waste by either being combusted for heat generation or just discarded [7].  
49 Recently, lignin-first biorefinery concept has been emphasized to make full use

50 of biomass. These studies are targeted at obtaining reactive lignins that could be  
51 used as the ideal candidate for catalytic depolymerization into aromatic  
52 monomers, such as phenol, guaiacol, 4-ethyltoluene and others [8]. This  
53 objective necessitates the preparation of lignin with a similar structure to the  
54 native lignin, *i.e.*, abundant  $\beta$ -O-4 bonds and few condensed structures. However,  
55 lignin isolation is still challenging due to its inherent heterogeneity, complexity,  
56 and the tendency to suffer from irreversible degradation and condensation  
57 reaction [9]. In recent years, several pretreatment solvents such as alkaline  
58 solution, organic solvents, and ionic liquids have been applied to fractionate good  
59 quality of lignin effectively. However, these methods have not fully addressed  
60 the aforementioned issues. Alkaline lignin showed a relatively abundance of  
61 impurities, low molecular weight uniformity, and condensed structure [10].  
62 Organosolv and ionic liquid lignins also frequently contain undesired lignin  
63 condensation products due to high temperature and acidic conditions [11,12]. In  
64 order to protect the intact lignin structure and prevent the condensed reactions,  
65 Shuai et al. [13] developed a formaldehyde stabilization strategy preserving  
66 lignin structure for near theoretical monomers yield in the subsequent  
67 hydrogenolysis. Despite the high conversion yield, using toxic 1,4-dioxane and  
68 formaldehyde is unavoidable during the processing. To replace these toxic  
69 solvents, alcohol solvent-based pretreatments have been also studied. For  
70 instance, Wen et al. [14] found that the ethanol solution pretreatment resulted in  
71  $\alpha$ -etherification of lignin side chains. Morteza et al. [15] also reported that  
72 glycerol incorporation could significantly prevent lignin condensation and lead  
73 to the preservation of  $\beta$ -O-4 linkage-rich lignin. These studies may offer a guide  
74 for the lignin-first strategy.

75 DES pretreatment has recently been considered a promising approach to  
76 dissociate and recover lignin (*i.e.* DESL), at the same time enhance the  
77 digestibility of the resulting substrates. DESL preparation features mild reaction  
78 conditions, high purity and uniformity [16,17]. Additionally, compared to  
79 traditional ionic solvents, DES is biocompatible, biodegradable, low-cost, and  
80 environmentally-friendly, significantly facilitating its application in biomass  
81 pretreatment [18]. DESs comprise at least one hydrogen bond acceptor (HBA)  
82 and one hydrogen bond donor (HBD) counterpart, forming a transparent liquid  
83 characterized by the low freezing point at mild conditions [19]. Previous studies  
84 [20,21] have illustrated that the glycosidic (C-O-C) bonds in both hemicellulose  
85 and lignin-carbohydrate complex (LCC) could be cleaved during DES  
86 pretreatment. Up to now, a large number of different DES systems such as using  
87 organic acid (ChCl/ lactic acid and ChCl/ formic acid), alcohol ((ChCl/ ethylene  
88 glycol and ChCl/ glycerin), and lignin-derived compounds (ChCl/*p*-  
89 hydroxybenzoic acid and ChCl/guaiacol) have been investigated [18,21].  
90 Typically, they can result in over 70% delignification and over 90% enzymatic  
91 saccharification. However, the structural integrity of the recovered lignin in  
92 reported articles is frequently significantly altered even under mild conditions  
93 [22]. For instance, Shen et al. [23] demonstrated that the  $\beta$ -O-4 linkages had been  
94 degraded from 69.52/100Ar (CEL) to 11.84/100Ar (110 °C) in the pretreatment  
95 of eucalyptus using ChCl/lactic acid. Wang et al. [24] also illustrated the  
96 significant degradation of  $\beta$ -O-4 bonds from 53.24/100Ar (CEL) to 5.35/100Ar  
97 (120 °C) in the pretreatment of hybrid *Pennisetum* using Lewis acid catalyzed  
98 ChCl/glycerol. Thus, these DES-induced lignin changes make it difficult to

99 utilize further. The exploitation of reactive lignin seems to be the key in the  
100 application of lignin-first DES pretreatment.

101 To avoid undesired lignin condensation in traditional DES pretreatment, we  
102 herein proposed to use 1,4-butanediol (BDO), a carbocation scavenger, as the  
103 HBD, with the aid of trace  $\text{AlCl}_3$ . With this system, a high level of delignification  
104 could be achieved at a relatively mild pretreatment condition. Heteronuclear  
105 single quantum coherence (HSQC) nuclear magnetic resonance (NMR) results  
106 revealed that this strategy significantly preserved the  $\beta$ -O-4 substructure without  
107 compromising lignin removal and glucan digestibility. The mechanism of the  
108 lignin protection during the pretreatment was systematically analyzed. To the  
109 best of our knowledge, this study for the first time reports the protection of the  
110 lignin's integrity during the DES pretreatment, which could increase the value of  
111 DES lignin and benefit the whole DES based biorefinery processing.

112 **2. Experimental section**

113 **2.1 Material preparation**

114 **2.1.1 Feedstock and chemicals preparation.**

115 Moso bamboo culms were provided by Xianhe Paper Industry Co. Ltd  
116 (Zhejiang Province, China). Bamboo culms were first immersed in tap water for  
117 12 h and then fibrillated by a twin-screw extruder (TSE). After being dewatered  
118 and air dried (containing 7.27% water), the crushed bamboo was stored at RT  
119 before use. Cellulase (CTec 2, Novozymes) and xylanase (X2753) were obtained  
120 from Sigma-Aldrich (Shanghai, China). All other chemicals were purchased  
121 from Macklin Biochemical Co., Ltd (Shanghai, China) and used as received.

122 **2.1.2 DES Synthesis, pretreatment and lignin recovery.**

123 We synthesized the DES by mixing  $\text{ChCl}$ , 1,4-BDO, and  $\text{AlCl}_3$  into a 500  
124 mL three-neck flask at a molar ratio of 25:50:1, and then heated in an oil bath at  
125 90 °C with constant agitation until forming a homogeneous and transparent  
126 liquid. The DES was sealed and stored in a desiccator for further use. For the  
127 DES pretreatment, 10 g dry biomass was mixed with 100 g DES in a three-neck  
128 flask which was then transferred into an oil bath at various temperatures of 80-  
129 140 °C for 1 h with constant agitation. After pretreatment, the mixture was  
130 immediately transferred into a 1 L beaker containing 300 mL of acetone/water  
131 (1:1, v/v). After magnetic stirring for 2 h, the mixture was vacuum filtrated and  
132 then washed with another 200 mL fresh acetone/water (v/v, 1:1) twice. The solid  
133 portion was further washed using DI water until neutral pH, then stored in a  
134 refrigerator for further analysis. The filtrate (including the additional 200 mL  
135 acetone/water) was collected and rotary-evaporated at 50 °C to remove the  
136 acetone. Next, 1 L DI water was introduced to regenerate the dissolved lignin  
137 fraction. Finally, the precipitated lignin was separated by centrifugation, and then  
138 water-washed three times, and freeze-dried. The dried lignin was sealed and then  
139 stored in a desiccator in dark for further study. After the lignin precipitation, the  
140 DES was recovered through rotary evaporation to remove the water at 70 °C, and  
141 the recovered DES was weighed to determine the recovery yield.

142 **2.2 Substrates characterization**

143 **2.2.1 Enzymatic hydrolysis**

144 Enzymatic hydrolysis was conducted in 150 mL flasks with a solid loading  
145 of 2.5% at a 20 mL working volume. In brief, 0.5 g (dry weight) of raw bamboo  
146 and pretreated substrates were weighed into the flasks, followed by 1 mL 1 M

147 acetate buffer to regulate the pH around 4.8. Cellulase (25 FPU/g-glucan) and  
148 xylanase (150 U/g-xylan) were then introduced. Finally, DI water was  
149 supplemented to provide a total volume of 20 mL. The sealed flasks were then  
150 transferred into a shaker (at 50 °C and 150 rpm), and incubated for 72 h. After  
151 enzymatic hydrolysis, an aliquot of 1 mL was taken for measuring the sugars  
152 output through the high-performance liquid chromatography (HPLC).

153 **2.2.2 Compositional analysis of raw and pretreated bamboo**

154 The chemical compositions of the samples in this study were analyzed in  
155 accordance with the procedure proposed by the National Renewable Energy  
156 Laboratory (NREL) [25]. Briefly, 0.3000 g samples (20-80 mesh) were first  
157 hydrolyzed with 3.0 mL of 72 (w/w)% sulfuric acid in a shaker (at 30 °C) for 1  
158 h. Water was then added to dilute sulfuric acid to 4 (w/w)%, which was finally  
159 autoclaved at 121 °C for another 1 h. All the monomeric sugars in this study were  
160 measured by high-performance liquid chromatography (Agilent 1260 series,  
161 Agilent Technologies, Santa Clara, CA) equipped with a Bio-Rad Aminex HPX-  
162 87H column.

163 **2.2.3 Substrates characterizations**

164 X-ray diffraction (XRD) studies were conducted on a Bruker Advanced D8  
165 diffractometer (Bruker, Germany) equipped with a Cu-K $\alpha$  X-ray generator at a  
166 40 kV voltage and a 40 mA current. The test was performed within 2 $\theta$  range of  
167 10°-40° at a 2°/min scanning rate. The crystallinity index (CrI) was calculated  
168 based on the flowing equation:

$$169 \quad CrI = \frac{[I_{002} - I_{am}]}{I_{002}} \times 100\%$$

170  $I_{002}$  is the maximum intensity of the diffraction peaks at  $\sim 18^\circ$ , and  $I_{am}$  is the  
171 minimum intensity at  $\sim 22^\circ$  of the amorphous portion [26].

172 Cellulose degree of polymerization was measured according to a viscosity  
173 procedure (termed as  $DP_v$ ). Prior to the test,  $\alpha$ -cellulose was acquired  
174 according to the method detailed in the supporting information. The limiting  
175 viscosity of the samples was measured through the ISO 5351 standard [27].  
176 First, 100 mg of completely dried sample was weighed into the flask, and then  
177 adding 10 mL DI water. The suspensions were mixed with magnetic stirring  
178 until it was completely dispersed. Then, 10 mL of bi(ethylenediamine) copper  
179 (II) hydroxide solution was added to dissolve  $\alpha$ -cellulose. Finally, the flasks  
180 were placed in a water bath ( $25^\circ\text{C}$ ) for the viscosity test with a Ubbelohde-  
181 viscosity meter. The measurement was performed in triplicate, and the final  
182 result represented an average. The  $DP_v$  values were calculated based on the  
183 limiting viscosity values using the flowing equation:

$$184 \quad DP_v = \left( \frac{0.75 \times [\eta]}{0.0050246256405154} \right)^{\frac{1}{0.905}}$$

185 Where  $[\eta]$  was obtained from the published study according to the  
186 correction parameter of the viscometer and the time interval between two scale  
187 lines.

188 Fourier transform infrared (FTIR) analysis was conducted to investigate the  
189 chemical structure variations of bamboo during the pretreatment. It was  
190 accomplished with a Bruker TENSOR27 spectrometer in transmittance mode  
191 with 32 scans at  $4\text{ cm}^{-1}$  resolution over the wavenumber range of  $4000\text{-}400\text{ cm}^{-1}$ .

192 Microstructure morphology of the original and pretreated bamboo was  
193 observed with a Hitachi 3400-N scanning electron microscope (Hitachi, Japan)

194 using a 15 kV accelerating voltage. Samples were first mounted on an aluminum  
195 stub through electric tapes and then spray-coated with gold.

196 **2.2.4 Lignin Characterization**

197 The lignin recovery yield was calculated based on the removed lignin after DES  
198 pretreatment, and the calculating equation was shown as follows:

$$199 \text{ Lignin recovery yield (\%)} = \frac{\text{Lignin recovered from the lignin - rich liquid (g)}}{\text{Total removed lignin from the initial bamboo (g)}} \times 100\%$$

200 Raw bamboo's cellulolytic enzyme lignin (CEL) was isolated by sequential  
201 enzymatic hydrolysis and dioxane extraction. The details of preparing CEL can  
202 be found in our previous publication [6]. Two-dimensional heteronuclear single  
203 quantum coherence nuclear magnetic resonance (2D-HSQC NMR) were  
204 performed through a Bruker Ascend<sup>TM</sup> 600 MHz spectrometer. The acquisition  
205 parameters were as follows: 166 ppm spectral width in F1 (<sup>13</sup>C) dimension with  
206 256 data points and 12 ppm spectral width in F2 (<sup>1</sup>H) dimension with 1024 data  
207 points, a J<sub>C-H</sub> of 145 Hz, a 1.0 s pulse delay, and 128 scans.

208 According to our previous study, the lignin hydroxyl groups were  
209 determined by <sup>31</sup>P NMR [6]. It was also performed on the Bruker 600 MHz  
210 instrument. In brief, oven-dried lignin samples (~20 mg) were dissolved in a  
211 solvent (~0.4 mL), which was composed of anhydrous pyridine and deuterated  
212 chloroform (1.6:1, v/v). chromium acetylacetonate and cyclohexanol were used,  
213 respectively, as the relaxation and internal standard. An excess amount of 2-  
214 chloro-4,4,5,5-tetramethyl-1,3,2-dioxaphospholane (TMDP) (~0.1 mL) was  
215 added as a phosphorylation reagent to react with the mixed solution. The mixture  
216 was immediately transferred into the NMR tube and then subjected to the test.

217 The regenerated lignin's microstructural changes and surface characteristics  
218 were observed with a field emission scanning electron microscopy (FE-SEM,  
219 Regulus 8100, Hitachi, Japan) working at 10 kV acceleration voltages. Prior to  
220 the SEM analysis, the samples were first oven-dried overnight at 50 °C. The dried  
221 samples were mounted on an aluminum stub through electric tapes and then sputter  
222 coated with gold.

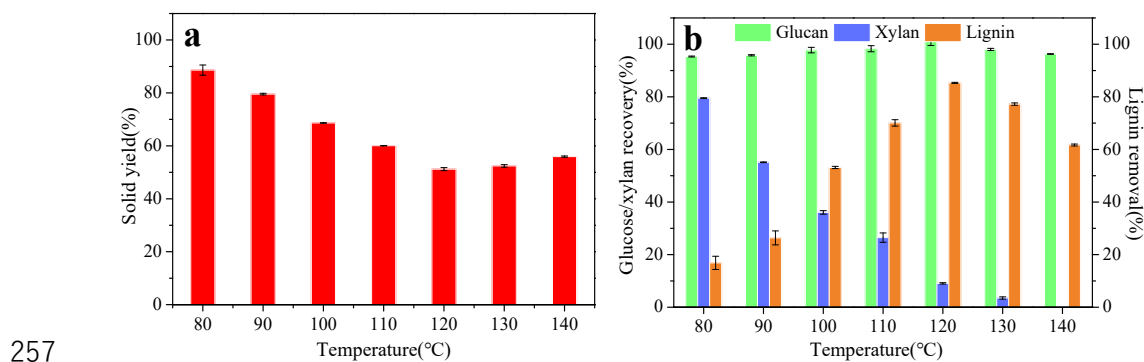
223 **3. Results and discussion**

224 **3.1 Substrates characterization**

225 **3.1.1 Compositional analysis of the raw and pretreated bamboo.**

226 This study adopted a twin-strew extruder to fibrillate the bamboo culms  
227 which is superior to the normal milling process in terms of the low energy  
228 consumption and ease to operation. The fibrillated bamboo was then subjected  
229 to the DES pretreatment and the solid recovery of the pretreated biomass is  
230 summarized in Fig. 1a. As shown, the solid recovery yield of the pretreated  
231 bamboo decreased from 88.63% to 51.20% with the pretreatment temperature  
232 increasing from 80 °C to 120 °C, indicating that more lignocellulose was  
233 dissolved as the pretreatment temperature increased. However, solid recovery  
234 increased from 51.20% to 55.95% when further increasing the temperature from  
235 120 °C to 140 °C. This was induced by the formation of pseudo lignin under  
236 severe condition [28], and further discussion will address this later. The recovery  
237 yields of glucan, xylan and lignin removal were calculated based on the dry  
238 weight of original and pretreated bamboo. As shown in Figure 1b, hemicellulose  
239 and lignin were readily removed from biomass solids during the DES  
240 pretreatment. At 80 °C, 79.39% hemicellulose was retained with 18.65%

241 delignification. As the pretreatment temperature increased, the recovery yield of  
 242 hemicellulose was reduced considerably from 79.39% (80 °C) to 55.02% (90 °C),  
 243 36.55% (100 °C), 27.74% (110 °C) and 8.88% (120 °C), and no hemicellulose  
 244 was detected using a temperature of 140 °C. At the same time, the delignification  
 245 efficiency was substantially increased from 18.65% (80 °C) to 85.45% (120 °C),  
 246 indicating the highly effective delignification by the proposed DES. However,  
 247 further increase of temperature beyond 120 °C decreased the lignin removal, with  
 248 values of 77.25% and 61.69% at 130 °C and 140 °C, respectively. This effect was  
 249 ascribed to the agglomeration of the dissolved lignin and the formation of pseudo  
 250 lignin that precipitated on the substrate surface. Nevertheless, the glucan  
 251 recovery yield was maintained at nearly 95% (94.29%-97.79%) during the  
 252 pretreatment, confirming that glucan was barely hydrolyzed or degraded  
 253 throughout the pretreatment. It should be noted that the sole ChCl/BDO without  
 254 the addition of AlCl<sub>3</sub> was incapable of removing xylan and lignin (data not  
 255 shown), even at high temperatures, indicating AlCl<sub>3</sub> as a key promoter in the  
 256 proposed DES [18].



257 258 **Fig. 1** Solid yield of substrates (a) and detailed components variations (b).

259

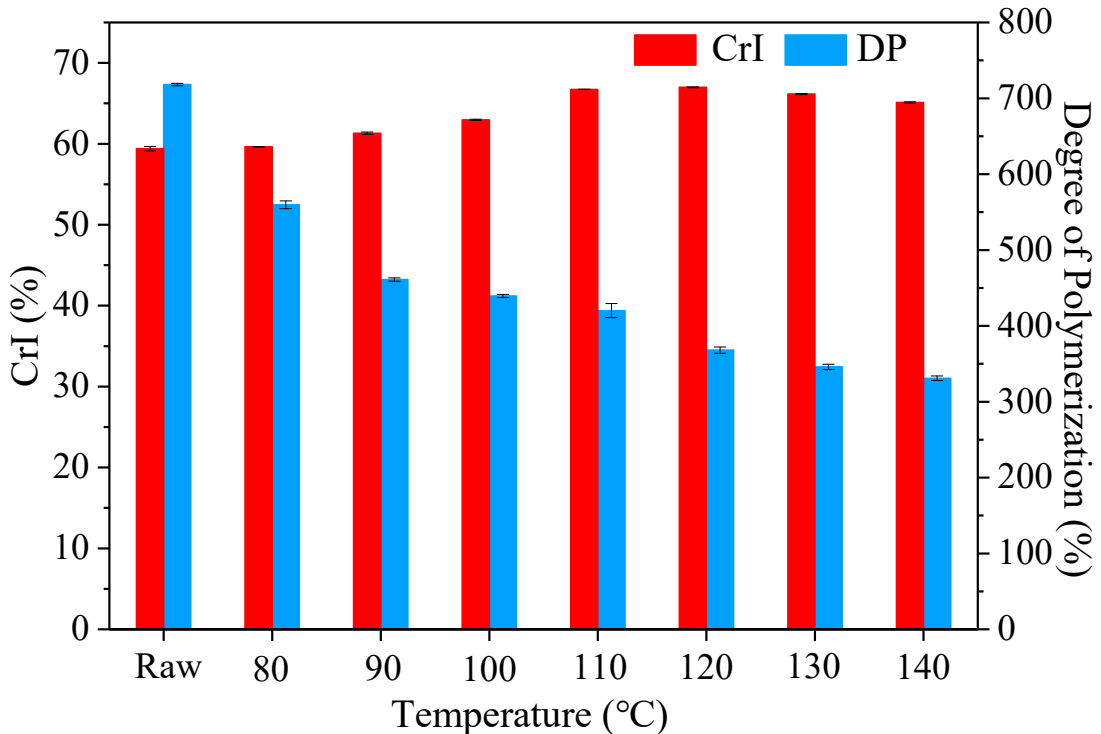
260 **3.1.2. SEM analysis of substrates before and after pretreatment**

261 SEM analysis was applied to investigate the microstructure changes of  
262 biomass during the DES pretreatment. As illustrated in Fig. S1, discernible  
263 variations of the bamboo fibers were observed during the pretreatment. The size  
264 of pretreated substrates decreased with the pretreatment temperature increasing.  
265 At 80 °C and 90 °C, the bamboo fiber length was close to that of the raw sample,  
266 and their surface was clear and smooth (Fig. S1b and c). When the DES  
267 pretreatments were performed at higher temperatures of 100-140 °C, the fiber  
268 length clearly decreased, and some cracks were evidently observed on the  
269 pretreated samples (Fig. S1e-h). Moreover, spherical-shaped and nub-like lignin  
270 debris were observed on the bamboo fibers' surface (see white arrows in Fig. S1).  
271 It has been widely reported that the small debris could be ascribed to the lignin  
272 migration of inner regions to the external surface, and the generation of pseudo  
273 lignin [23].

274 **3.1.3 Impact of the pretreatment on the substrates crystallinity and cellulose  
275 degree of polymerization (DP<sub>v</sub>)**

276 The CrI (crystalline index) of the original and pretreated bamboo are shown  
277 in Fig. 2. The CrI of the untreated bamboo was 59.63%, and it gradually  
278 increased to 67.03% with the temperature increasing from 80 to 120 °C. This  
279 change was mainly ascribed to the removal of amorphous lignin and  
280 hemicellulose throughout the pretreatment. After that, the CrI of pretreated  
281 bamboo slightly decreased from 67.03% to 65.17% with the temperature  
282 increasing from 120 to 140 °C, which was possibly due to the swelling effect on  
283 the crystalline zone induced by the permeation of DES solvent under harsher  
284 reaction conditions [26].

285



286  
287 **Fig. 2** The CrI of substrates and cellulose DP<sub>v</sub> from original and pretreated  
288 bamboo

289  
290 Cellulose DP<sub>v</sub> is another important character affecting cellulose  
291 saccharification. As shown in Fig. 2, the cellulose DP<sub>v</sub> of raw bamboo was 718,  
292 clearly lower than woody biomass like poplar and eucalyptus, which is because  
293 of the abundance of short parenchyma cells in bamboo [6]. Following the  
294 pretreatment, the cellulose DP<sub>v</sub> was significantly decreased to 559, 461, 439, 420,  
295 368, 346, and 330 as the temperature increased from 80 °C to 140 °C. The results  
296 indicated that the DES could cleave the glycosidic bond in cellulose and expose  
297 more reducing ends that facilitate the enzymatic hydrolysis of the substrates.

298 **3.1.4 FTIR spectroscopy analysis of the raw and the pretreated bamboo**

299 FTIR spectroscopy is widely employed in investigating the structure  
300 changes of the raw and pretreated substrates. As shown in Fig. S2, peaks at 896,  
301 1101, 1056 and 1426 cm<sup>-1</sup> are ascribed to C-O-C stretching in amorphous

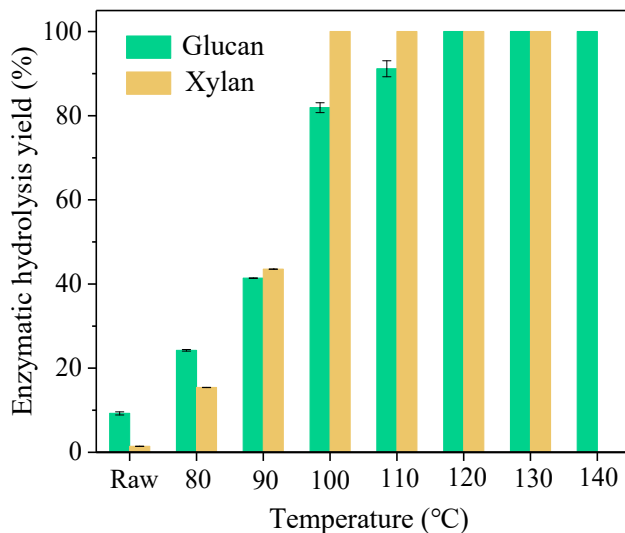
302 cellulose, C-O vibration in crystalline cellulose, C-O stretching of cellulose, C-  
303 H stretching of cellulose and C-H deformation (asymmetric) of cellulose [29].  
304 Clearly, these signals significantly increased after the pretreatment, indicating  
305 cellulose enrichment in the pretreated biomass solid. Additionally, the peak at  
306 1730 cm<sup>-1</sup>, which is assigned to carbonyl groups in branched hemicellulose, was  
307 observed to be weakened with increasing pretreatment temperature and  
308 eventually disappeared at 130 and 140 °C, this is caused by hemicellulose  
309 removal and the degradation of LCC (lignin-carbohydrate complex) structures  
310 [30]. In addition, the peaks at 1602 and 1507 cm<sup>-1</sup> correspond to aromatic skeletal  
311 vibration of lignin, and the peak at 1237 cm<sup>-1</sup> was assigned to the C-O vibration  
312 of the guaiacyl ring of lignin [29]. The intensity of these peaks became  
313 inconspicuous, especially under severe DES pretreatment conditions, which was  
314 attributed to the lignin removal. However, the peak at 1315 cm<sup>-1</sup> relating to C-O  
315 vibration in syringyl ring of lignin became conspicuous with increasing  
316 pretreatment temperature. This result revealed that the G unit was more readily  
317 removed from biomass in the pretreatment.

318 **3.1.5 Enzymatic digestibility of the raw and pretreated bamboo**

319 Enzymatic hydrolysis was performed to evaluate the impact of the DES  
320 pretreatment on sugar release. As shown in Fig. 3, after 72 h enzymatic  
321 hydrolysis, the saccharification yield of glucan and xylan of the raw bamboo was  
322 only 9.25% and 1.43%, respectively. After the DES pretreatment, the enzymatic  
323 hydrolysis was considerably enhanced. Specifically, the glucan saccharification  
324 yield was increased from 9.25% (raw substrate) to 24.24%, 41.40%, 81.92%,  
325 91.16% and 100% at temperatures of 80, 90, 100, 110, and 120 °C, respectively.  
326 The same trend was also found in the xylan digestibility which increased from

327 1.43% to 100%. Remarkably, the glucan hydrolysis yield ranged from 41.40% to  
328 100% as the temperature increased, 4 to 11 times higher than that of the raw  
329 bamboo. Generally, hemicellulose and lignin in the cell wall are two factors  
330 inhibiting enzymatic digestibility, in which they are crosslinked with each other,  
331 forming a networked structure that covers the cellulose. Moreover, non-  
332 productive adsorption of lignin to the enzyme generates a lignin-enzyme  
333 complex, which also significantly lowers saccharification efficiency [31]. To  
334 evaluate the importance of hemicellulose and lignin removal, the relationship  
335 between glucan saccharification ratio and the removal of lignin and xylan was  
336 characterized. As shown in Fig. S3, a strong linear correlation between the glucan  
337 hydrolysis yield and lignin removal ( $R^2=0.9451$ ) as well as xylan removal  
338 ( $R^2=0.9386$ ) was observed, implying that the removal of both lignin and  
339 hemicellulose highly reduced the recalcitrance and thus significantly improved  
340 saccharification efficiency.

341 Furthermore, as described in Fig. S4, a strong negative correlation between  
342 the glucan hydrolysis yield and  $DP_v$  ( $R^2=0.8624$ ) was also observed. This result  
343 indicated that the enzymatic hydrolysis yield was significantly enhanced with the  
344 decrease of cellulose  $DP_v$ , which was induced by the depolymerization of  
345 cellulose chains, thus increasing the specific surface area of cellulose and  
346 exposing more reducing ends [32].



347

348 **Fig. 3** Glucan and xylan saccharification yields of the raw and the DES pretreated  
 349 bamboo under different pretreatment temperatures.

350

### 351 3.2 Lignin characterization

#### 352 3.2.1 Carbohydrates Analysis of Regenerated Lignin.

353 As shown in Fig. S5, the recovery yield of the DES-induced lignin was over  
 354 80% for all the pretreatment runs (except 80 °C), which was significantly higher  
 355 than conventional pretreatment methods such as alkaline and some organosolv  
 356 processes [33-35].

357 Compositional analysis was performed to investigate the purity of these  
 358 regenerated lignins. As shown in Table S1, only trace carbohydrates were  
 359 detected (less than 0.3% glucan and 2.01% xylan). In addition, with the  
 360 pretreatment temperature increasing, the amount of the associated carbohydrates  
 361 declined, and they were barely detected at temperature higher than 120 °C,  
 362 indicating the high purity of our regenerated lignin. The nearly pure lignin

363 prepared in this study is favorable for the lignin valorization, such as catalytic  
364 depolymerization and nanocomposites manufacturing.

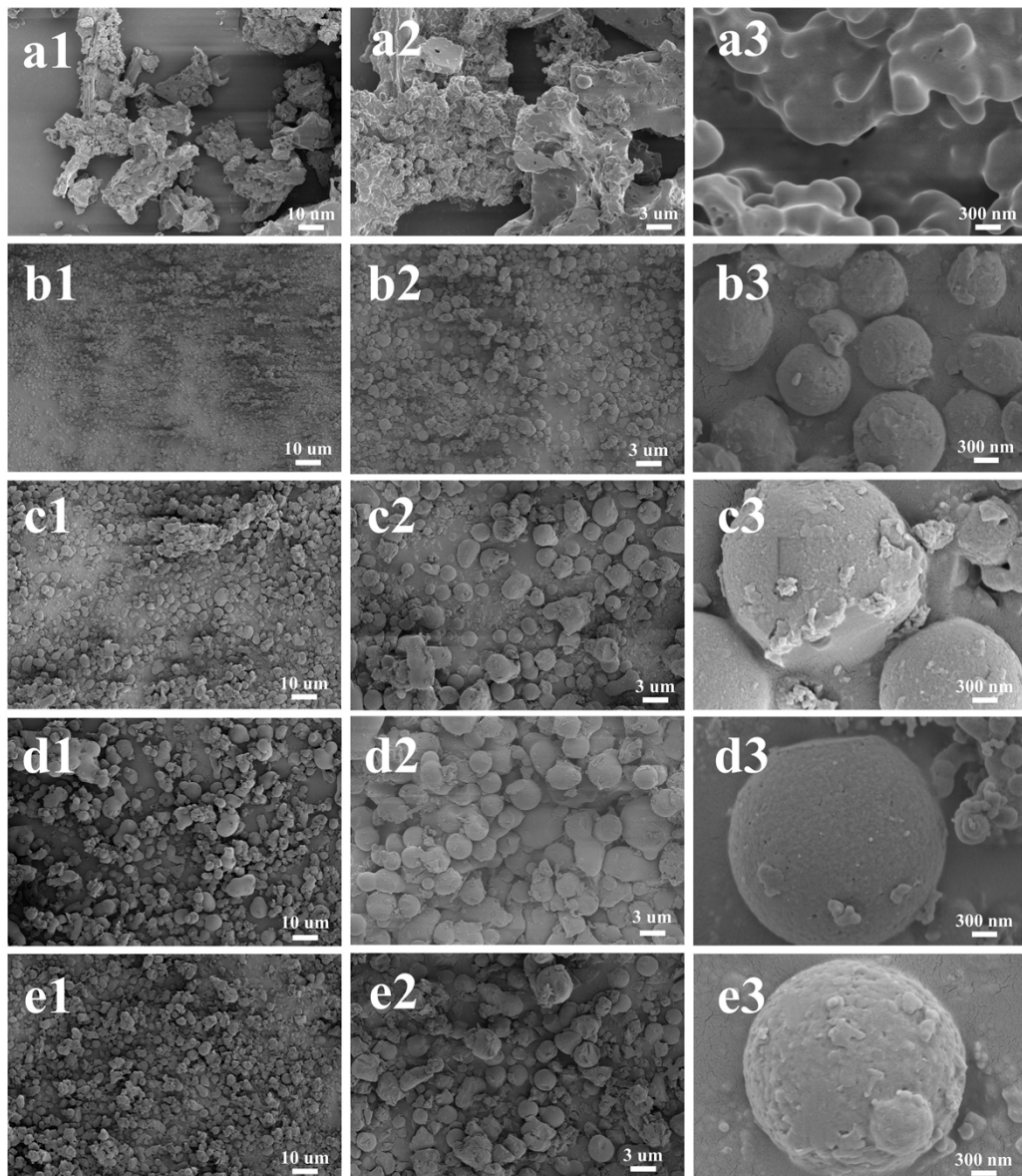
365 **3.2.2 FTIR spectroscopy analysis of the original CEL and regenerated lignin**

366 The lignin of the original and regenerated lignin exhibited similar FTIR  
367 spectra, indicating the structural integrity of the regenerated lignins (Fig. S6).  
368 The characteristic signals at  $\sim 1700$   $\text{cm}^{-1}$  attributed to C=O stretching vibrations  
369 in carbonyls, non-conjugated ketones, and ester of lignin groups [36] were  
370 strikingly enhanced as the pretreatment strengthened. Additionally, the  
371 absorption bands at 1602, 1459 and 1513  $\text{cm}^{-1}$  corresponded to the lignin  
372 aromatic skeleton have no significant variation [37]. This data implied that the  
373 aromatic skeleton of regenerated lignin was not significantly disintegrated during  
374 the treatment. Further, the peaks at 1148, 1032 and 1357  $\text{cm}^{-1}$  attributed to the  
375 characteristic signals of guaiacyl unit [38] were weakened in all the runs. The  
376 peak at 1255  $\text{cm}^{-1}$  corresponded to syringyl unit, and the peak at 832  $\text{cm}^{-1}$  related  
377 to *p*-hydroxyphenyl (H) unit [36] indicated no significant change with the  
378 temperature increasing. These results suggested that the regenerated lignin  
379 contains more S units but less than G units, and the 2D-HSQC NMR analysis  
380 further confirms this.

381 **3.2.3 Morphology of the regenerated lignins**

382 The morphological features of the CEL and recovered lignin were  
383 investigated *via* SEM, as shown in Fig. 4. The CEL featured as irregular and  
384 lump-shaped agglomerates, which is composed of interconnected and  
385 homogeneous ellipse-like particles. Interestingly, after our DES pretreatment, all  
386 the regenerated lignin had a spherical shape. DES lignin in previous article was  
387 in flake-like or unregular shapes [39]. Uniquely, herein, the BDO DES generated

388 lignins with a regular sphere shape. The size of the lignin spheres was observed  
389 to be several microns and it seems to be enlarged with increasing the temperature.  
390 The possible mechanism of generating the regular spherical lignin was proposed (Fig.  
391 S7) [40]. In brief, after adding water to the lignin-abundant DES, lignin nuclei were  
392 formed through aggregating the large and homogenous hydrophobic lignin, and then  
393 the nuclei gradually grew into micro spherical lignin through absorbing the small lignin  
394 particles, which formed a hydrophobic nucleus and a hydrophilic shell. During the  
395 nucleation process, lignin started to aggregate through the hydrophobic interaction  
396 which formed stable nuclei, and the surface of the nuclei was hydrophilic. After that,  
397 the hydrophilic lignin debris adsorbed onto the surface of the nuclei, thus promoted the  
398 nuclei to grow into micro spherical lignin. Besides, the BDO grafted onto the  $\alpha$ -position  
399 of lignin aliphatic side chain during our DES pretreatment could increase the  
400 hydrophilicity of the lignin, which further promoted the swelling growth process of the  
401 lignin spheres. Further studies concerning the mechanism and application of the lignin  
402 microspheres are ongoing and will be reported in our future studies.



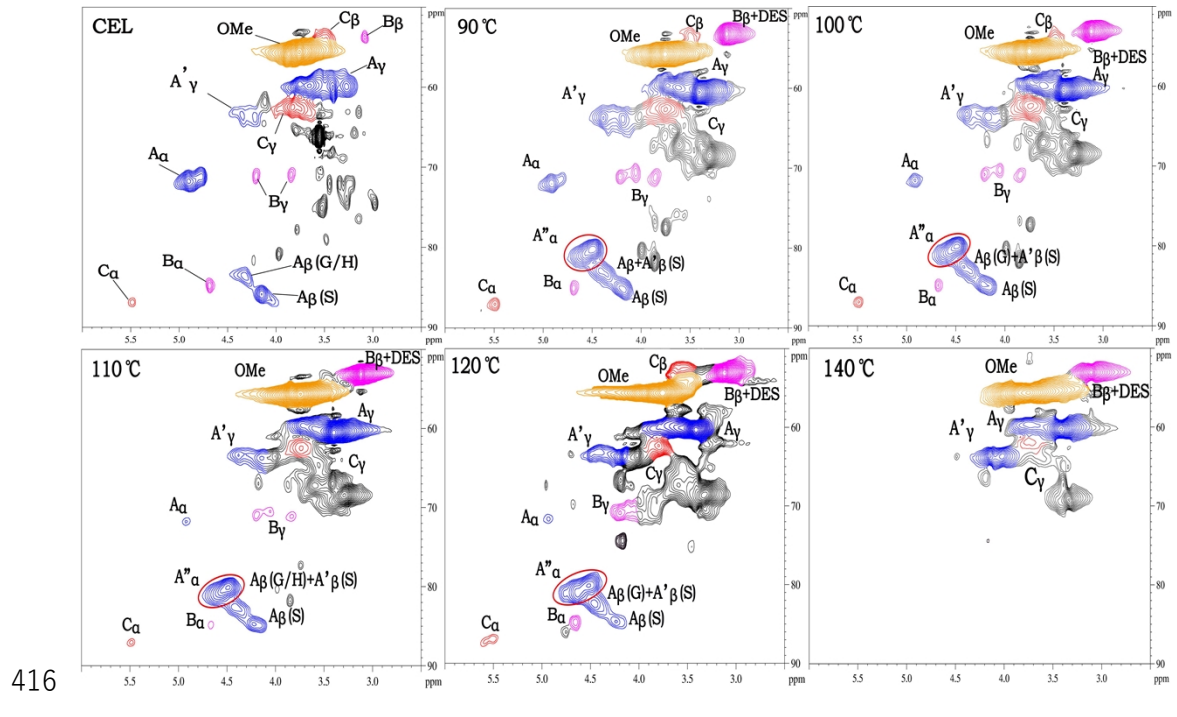
404 **Fig.4** SEM images of CEL (a1-a3), recovered lignins at different temperatures  
 405 of 90 °C (b1-b3), 100 °C (c1-c3), 120 °C (d1-d3), and 140 °C (e1-e3).

406

407 **3.2.4 HSQC NMR analysis of CEL and recovered lignin**

408 For the detailed structural information of the recovered lignins in different  
 409 pretreatment conditions, 2D-HSQC NMR analysis was conducted. CEL was  
 410 prepared as a control to observe the structural changes during the pretreatment  
 411 process. The side-chain ( $\delta_C/\delta_H$  50.0-90.0/2.50-6.0 ppm) and aromatic ( $\delta_C/\delta_H$   
 412 100.0-150.0/9.0-5.5 ppm) regions of the HSQC spectra of the regenerated lignins

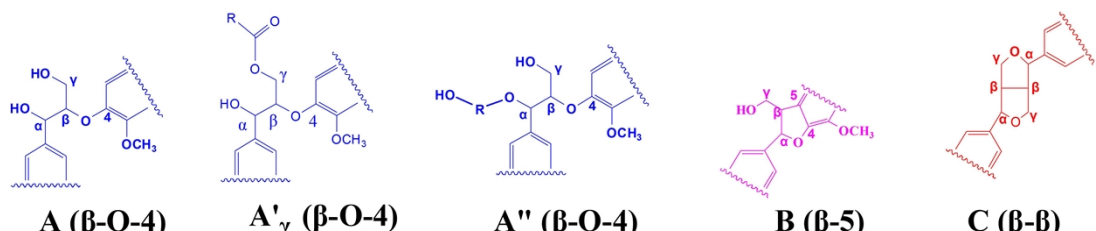
413 are shown in Fig. 5 and Fig. 6. The main lignin cross-signals of the 2D-HSQC  
 414 spectra, as demonstrated in Table S2, were referred to the previous publications  
 415 [23,39,41].



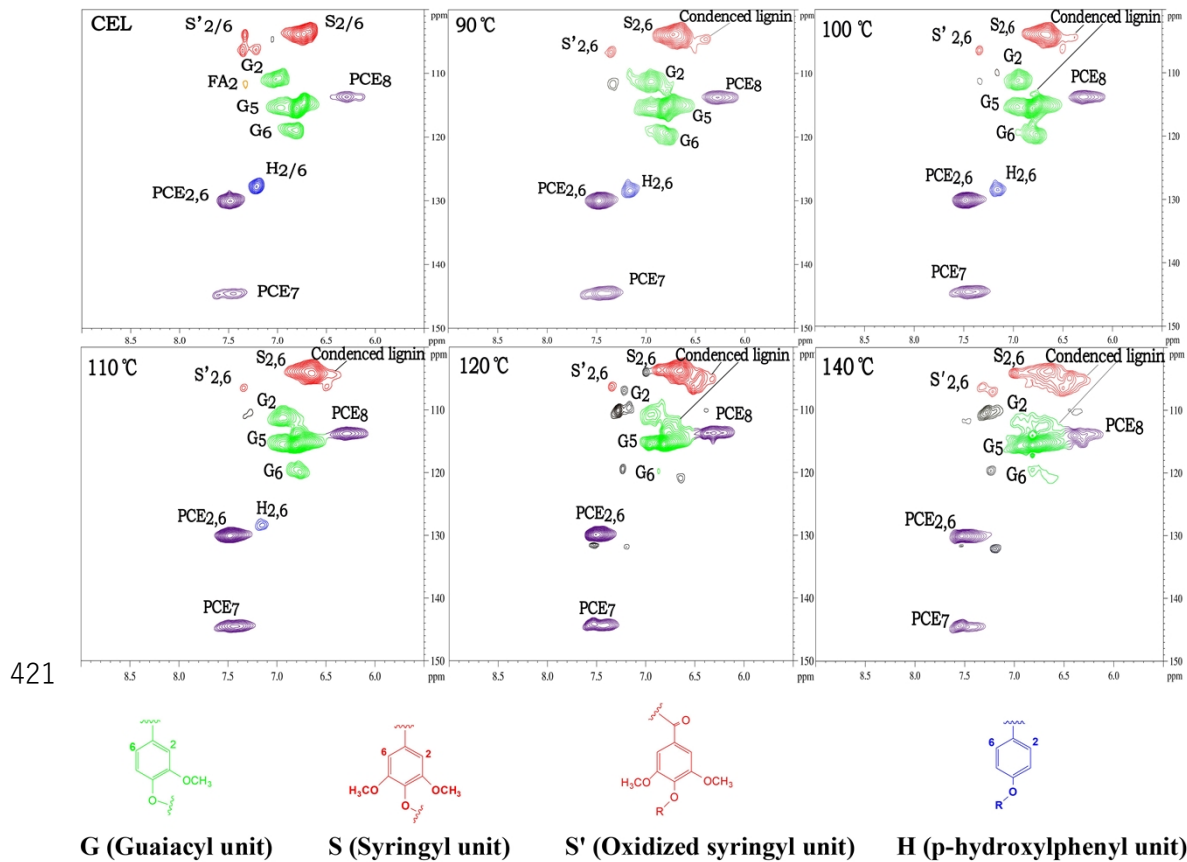
416

417

418



419 **Fig. 5** Side-chain regions of CEL and the regenerated lignin fractions in the 2D-  
 420 HSQC NMR spectra under different pretreatment temperatures.



422 **Fig. 6** Aromatic regions of the CEL and regenerated lignin fractions in the 2D

423

424 **Fig. 6** Aromatic regions of the CEL and regenerated lignin fractions in the 2D

425 HSQC NMR spectra under different pretreatment temperatures.

426

427 In the side-chain region (Fig. 5), CEL showed pronounced signals of  $\beta$ -O-4

428 ( $A_\alpha$ ),  $\beta$ - $\beta$  ( $B_\alpha$ ), and  $\beta$ -5 ( $C_\alpha$ ) linkages at 71.62/4.85, 84.73/4.65, and 86.83/5.42

429 ppm. Additionally, the  $\gamma$ -acetylated  $\beta$ -O-4 linkages ( $A_\gamma'$ ) were also observed,

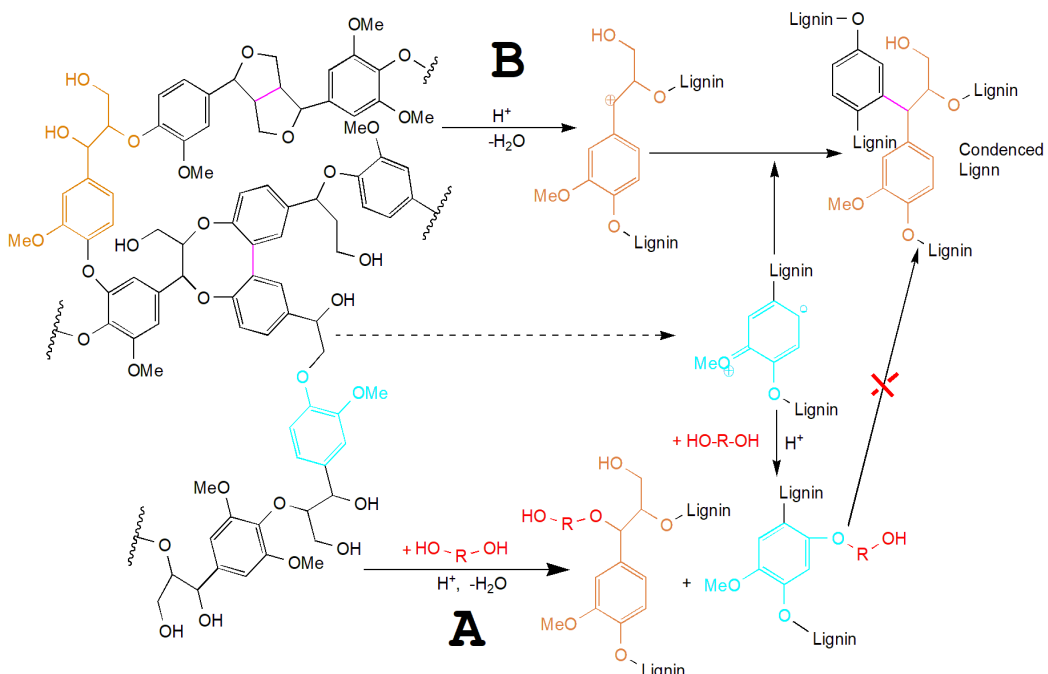
430 indicating the existence of LCC structure in bamboo [42]. After the DES

431 pretreatment, the  $A_\alpha$  signal of regenerated lignin was weakened even at the mild

432 temperature of 90 °C. Meanwhile, a new signal was discovered at 80.05/4.49

433 ppm in the recovered lignin HSQC NMR spectra (see red rings in Fig. 5). This

434 data was assigned to  $\beta$ -O-4 structure derivatives ( $A''_a$ ) which is caused by the  
435 graft of 1,4-BDO onto the  $\alpha$ -position of the  $\beta$ -O-4 linkage (Fig. 7, route A)  
436 [16,31]. During the pretreatment, the position of the  $\beta$ -O-4 structure was  
437 hydrolyzed to form a positively charged carbon by the departure of leaving  
438 groups, which normally lead to the condensation in most cases (Fig. 7, route B).  
439 However, in this study, 1,4-BDO acted as a nucleophile to attack the carbocation  
440 intermediates, forming the  $\alpha$ -etherified lignin that suppressed the condensation  
441 [16,43]. In addition, as shown in Fig. S8, lignins regenerated at the temperature  
442 lower than 110 °C all exhibited a brown color, similar to native CEL, and in  
443 evident contrast to lignin recovered from severe conditions of L140 °C, which  
444 has a very dark color, suggesting more condensed structures [44]. As expected,  
445 the proposed DES system protected the lignin structure and preserved  $\beta$ -O-4  
446 linkage in regenerated lignins (Table 1). The  $\beta$ -O-4 bond content in regenerated  
447 lignins was as high as 59.06/100Ar (90 °C), 51.95/100Ar (100 °C), and  
448 46.47/100Ar (110 °C), which is close to the native CEL (59.19%). Previous  
449 reports concerning DES pretreatment only focused on the delignification and  
450 lignin recovery, while the lignin quality was not considered as much as the  
451 quantity [18,45,46]. In this study, we proposed a novel strategy by introducing  
452 carbocation scavenger into the DES system, which generated lignins possessing  
453 a similar structure to the native lignin. Even at the temperature of 120 °C,  $\beta$ -O-4  
454 bond content can still reach 31.82%, indicating a strong protective effect of our  
455 system. Nevertheless, no aryl ether was detected when further increasing  
456 temperature to 140 °C. In the case of  $\beta$ - $\beta$  and  $\beta$ -5, they were barely affected  
457 during the DES pretreatment except that at 140 °C where no  $\beta$ - $\beta$  or  $\beta$ -5 was  
458 found.



462 **Fig. 7.** Lignin extraction in normal case (route B), and the lignin protection by our DES  
463 (route A).

465 In the aromatic region (Fig. 6), guaiacyl (G), syringyl (S), and *p*-  
466 hydroxyphenyl (H) units signals were clearly recognized in bamboo CEL.  
467 Besides, the signals of oxidized syringyl units (S'), *p*-coumaric acid (*p*-CE), and  
468 ferulic acid (FA) were also unambiguously observed. After the DES  
469 pretreatment, no distinct signals shift of the S<sub>2,6</sub> and G<sub>5</sub> was observed with  
470 increasing temperature. This result is possibly due to the quenching of the  $\alpha$   
471 position of the  $\beta$ -O-4 structure by the 1,4-BDO, thus reducing the condensation  
472 reaction [31]. As to the content of FA, which existed as the LCC linkages, it  
473 gradually decreased and finally disappeared at temperature higher than 110 °C.  
474 On the contrary, the *p*-CE was almost unaffected by the pretreatment. For more  
475 detailed information about the lignin structure changes after the DES  
476 pretreatment, the main constituents of the ratio of S/G were calculated based on

477 the previous study method [47]. As shown in Table 1, the contents of S and G  
 478 units of bamboo CEL were 43.39/100Ar and 45.82/100Ar, respectively. With the  
 479 pretreatment temperature increasing, the S/G gradually increased and reached  
 480 1.16 at 140 °C. Notably, although the protection of the 1,4-BDO, some lignin  
 481 condensation was also observed during the pretreatment. Minimal lignin  
 482 condensation occurred at a low reaction temperature (up to 110 °C). The  
 483 condensed S unit increased from 6.35 to 9.10/100Ar (accounting for 14.07%-  
 484 19.87% of the total S unit, see Table 1), and condensed G unit was barely  
 485 observed. Further increasing the temperature, lignin condensation reactions were  
 486 increased. Finally, at 140 °C, 29.18/100Ar condensed S unit was observed,  
 487 accounting for 53.01% of the total S unit, and all the G unit was transformed into  
 488 the condensed form. This result confirmed the conclusion above that our strategy  
 489 could perform well at various temperatures (lower than 120 °C), which protects  
 490 the lignin structure with minimal sacrifice to delignification.

491 **Table 1.** Quantification of CEL and Regenerated Lignin (results expressed as per  
 492 100 Ar).

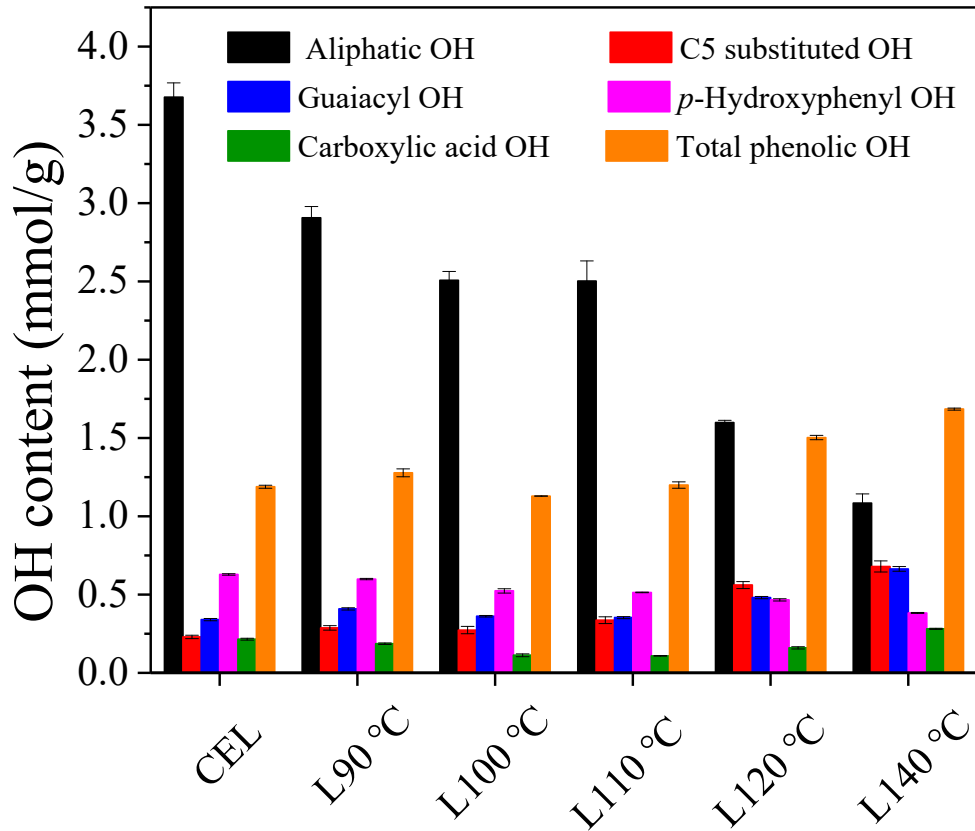
Sample	Lignin removal (%)	Lignin yield (%)	S		G		S/G	β-O-4	β''-O-4
			Total	Condensed	Total	Condensed			
CEL	-	-	43.39	0	45.82	-	0.95	59.19	0
L90 °C	26.35	79.00	45.13	6.35	46.91	1.14	0.96	18.83	40.23
L100 °C	53.15	83.01	45.66	7.74	45.94	1.99	0.99	14.65	37.30
L110 °C	70.10	86.49	45.79	9.10	47.74	2.54	0.96	9.37	37.10
L120 °C	85.30	85.11	52.30	16.67	47.70	10.24	1.10	5.96	25.86
L140 °C	61.69	89.18	55.0	29.18	44.95	44.95	1.16	-	-

493

494 **3.2.5 Quantitative  $^{31}\text{P}$  NMR analysis of the CEL and recovered lignins**

495 The changes of OH groups including aliphatic, phenolic, and carboxylic  
496 acid OH before and after DES pretreatments were investigated by  $^{31}\text{P}$  NMR.  
497 According to a previous publication, the peaks of syringyl OH and other  
498 condensed 5-substituted phenolic OH are overlapped in the NMR spectra;  
499 therefore, they are counted together as the C<sub>5</sub>-substituted phenolic OH content  
500 [6]. As shown in Fig. 8, in CEL, the aliphatic OH group, with a content of 3.61  
501 mmol/g representing 58.38% of the total OH groups, is dominant. After our DES  
502 pretreatment at 90, 100 and 110 °C, the aliphatic OH contents slightly decreased  
503 but still dominate the OH content (with content of 2.85 mmol/g at 90 °C, 2.47  
504 mmol/g at 100 °C and 2.59 mmol/g at 110 °C). It was also determined that the  
505 total phenolic OH was almost unchanged at these temperatures. These results  
506 supported the HSQC NMR result indicating that the β-O-4 structure was  
507 protected successfully during the extraction at low temperatures. Besides, the C<sub>5</sub>  
508 substituted units representing the condensed lignin OH varied from 0.29 (90 °C)  
509 to 0.26 (100 °C) and 0.32 mmol/g (110 °C), this slight variation of C<sub>5</sub> substituted  
510 units also suggested that our DES could sufficiently suppress the lignin  
511 condensation. However, when the pretreatment temperature was further  
512 increased from 110 °C to 140 °C, the aliphatic OH contents decreased  
513 significantly from 2.59 (110 °C) to 1.61 (120 °C) and 1.04 mmol/g (140 °C),  
514 while the phenolic OH increased from 1.19 (110 °C) to 1.49 (120 °C) and 1.69  
515 mmol/g (140 °C), and the C5 substituted OH increased from 0.32 (110 °C) to  
516 0.55 (120 °C) and 0.65 mmol/g (140 °C). These results indicate the β-O-4

517 structure was partially ruptured which increased the relative contents of phenolic  
518 OH compared to the aliphatic OH, accompanied by more condensed reactions  
519 occurring under harsher pretreatment conditions.



520  
521 **Fig. 8** Quantification of different OH groups in CEL and regenerated lignins by  $^{31}\text{P}$   
522 NMR.

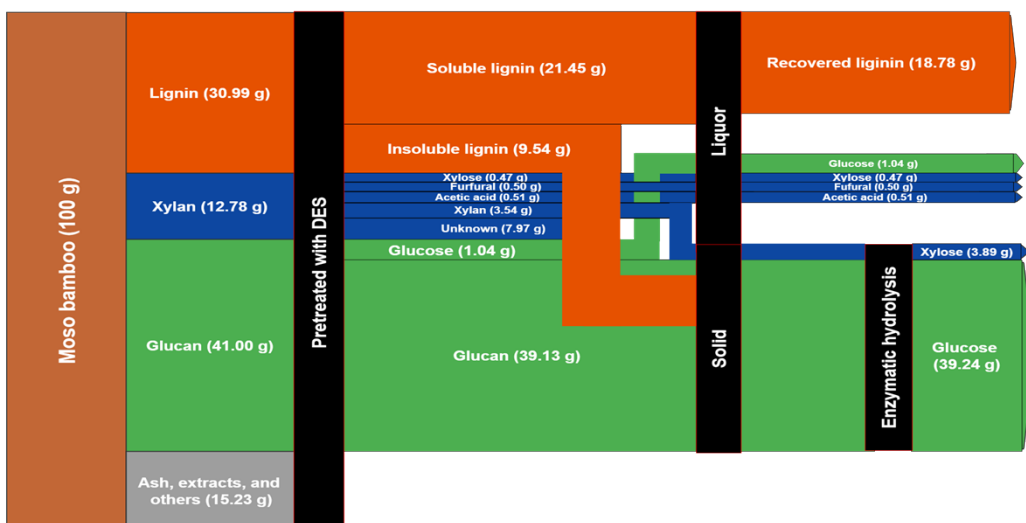
523

### 524 3.3 DES reuse and mass balance

525 The recyclability of the DES has been deemed as a main promoter for the  
526 DES-based lignocellulose pretreatment. Our studies demonstrated that the BDO  
527 DES showed excellent recyclability, as shown in Fig. S9. After recovery and  
528 testing seven times at 120 °C for 1 h, over 90% of DES could be recovered in  
529 each recycling stage. Besides, the lignin removal and the enzymatic hydrolysis  
530 yield were also investigated. It can be seen that the lignin removal gradually  
531 decreased but still maintained at ~70% in 2-4 cycles; thereafter, it decreased

532 suddenly and finally was 42.78% after the 7<sup>th</sup> circulations. Nevertheless, the  
533 glucan enzymatic hydrolysis yield in all the cycles could still reach 100% even  
534 after the 7<sup>th</sup> circulation (Fig. S10).

535 The mass balance after DES pretreatment (based on 100 g raw bamboo) is shown  
536 in Fig. 9. The raw bamboo contains 41.00 g glucan, 12.78 g xylan, and 30.99 g  
537 lignin. After DES pretreatment, the recovery of xylan in the pretreated solid was  
538 3.54 g which was completely hydrolyzed into xylose by enzymes. Furthermore,  
539 0.42 g of xylan was depolymerized into xylose during cooking which was  
540 accompanied with 0.51 g acetic acid and 0.50 g furfural. As to the regenerated  
541 lignin, 18.78 g lignin was recovered and possessed well-preserved structure.  
542 Furthermore, the glucan recovery approached a theoretical maximum yield of  
543 39.13 g, which could be enzymatically hydrolyzed into glucose (39.24 g). It is  
544 worth noted that the DES could be recovered with a 94.24% yield after separation  
545 of the solid and liquid, which will make the process sustainable and renewable.



547 **Fig. 9** Schematic diagram and mass balance of the proposed biorefinery sequence.

548

549 **4. Future perspectives**

550        Although the pretreatment approaches discussed above showed excellent  
551 ability to obtain lignins with well-preserved structures, as well as a high  
552 saccharification yield of glucan, the exploitation of hemicellulose remains to be  
553 determined. Under the acid DES, xylan is liable to degrade and generate xylose as the  
554 first production [48,49]. Further, xylose could be easily transformed into xylulose, and  
555 the xylulose normally dehydrates and generates furfural owing to the low activation  
556 energy. At more severe conditions, furfural could be transformed into furfuryl alcohol,  
557 and then produce levulinic acid through a ring-opening reaction. In addition, there is  
558 another degradation route of xylan, in which xylulose was transformed into  
559 glycolaldehyde and glyceraldehyde through anti-aldol condensation [50]. Next, the  
560 glyceraldehyde could dehydrate into methylglyoxal. At more sever condition, the  
561 methylglyoxal further transformed into methylglyoxal, formaldehyde, acetaldehyde,  
562 1,1-dihydroxy acetone, acetic acid, lactic acid and formic acid.

563        In this study, a minimal amount of furfural was detected. However, a series  
564 of other hemicellulose degradation chemicals such as acetic acid, levulinic acid,  
565 and lactic acid were detected after the DES pretreatment (see Table S4), which  
566 made the conversion of hemicellulose intractable and complicated. We could not  
567 even make a mass balance of hemicellulose, which indicates that other unknown  
568 intermediate products (such as methylglyoxal, acetaldehyde, glycolaldehyde,  
569 glyceraldehyde, 1,1-dihydroxy acetone, and methylglyoxal) existed in the  
570 system. We also discovered that the accumulation of lactic acid was remarkably  
571 increased from 0 (1<sup>st</sup> circulation) to 4.91 g/L (7<sup>th</sup> circulation). This may be  
572 induced by the transformation of xylose to lactic acid during the AlCl<sub>3</sub> assisted  
573 DES system [50], but it only showed a very low yield in this study. Therefore,  
574 future research endeavors should be directed towards hemicellulose valorization,

575 which could help to develop a tailor-made pretreatment process for desired  
576 products from the whole biomass and thus contribute to the sustainable  
577 biorefinery configuration.

578 **5. Conclusions**

579 This study systematically investigated the pretreatment of bamboo using a  
580 diol-based DES, reaching over 80% lignin removal while preserving almost all  
581 glucan. Besides, the hydrolysis digestibility of the substrate was significantly  
582 improved after the pretreatment. Importantly, the regenerated lignin possessed  
583 quite an intact structure with very high  $\beta$ -O-4 content (31.82%-59.19%), which  
584 is beneficial to the downstream lignin processing. Finally, the DES showed  
585 excellent recyclability even after the seven circles.

586 **Conflicts of interest**

587 There are no conflicts to declare.

588 **Acknowledgements**

589 This work was supported by Jiangsu Province Key Laboratory of Biomass  
590 Energy and Materials (JSBEM-S-202004), National Natural Science Foundation  
591 for Youth (32001273), and Young Elite Scientist Sponsorship Program by CAST.  
592 AJR and XM were supported by the University of Tennessee. CGY was  
593 supported by the State University of New York College of Environmental  
594 Science and Forestry Startup package.

595 **References**

596 [1] A. Mittal, R. Katahira, B.S. Donohoe, B.A. Black, S. Pattathil, J.M. Stringer,

597 G.T. Beckham, Alkaline Peroxide Delignification of Corn Stover, ACS  
598 Sustain. Chem. Eng. 5 (2017) 6310–6321.

599 [2] S.A. Rollag, J.K. Lindstrom, R.C. Brown, Pretreatments for the continuous  
600 production of pyrolytic sugar from lignocellulosic biomass, Chem. Eng. J. 385  
601 (2020) 123889.

602 [3] H. Bian, M. Dong, L. Chen, X. Zhou, R. Wang, L. Jiao, X. Ji, H. Dai, On-  
603 Demand Regulation of Lignocellulosic Nanofibrils Based on Rapid  
604 Fractionation Using Acid Hydrotrope: Kinetic Study and Characterization,  
605 ACS Sustain. Chem. Eng. 8 (2020) 9569–9577.

606 [4] C. Liu, Y. Deng, S. Wu, H. Mou, J. Liang, M. Lei, Study on the pyrolysis  
607 mechanism of three guaiacyl-type lignin monomeric model compounds, J.  
608 Anal. Appl. Pyrolysis. 118 (2016) 123–129.

609 [5] L. Xu, S.J. Zhang, C. Zhong, B.Z. Li, Y.J. Yuan, Alkali-Based Pretreatment-  
610 Facilitated Lignin Valorization: A Review, Ind. Eng. Chem. Res. 59 (2020)  
611 16923–16938.

612 [6] C. Huang, G. Fang, Y. Zhou, X. Du, L. Yu, X. Meng, M. Li, C.G. Yoo, B.  
613 Chen, S. Zhai, Q. Guan, Q. Yong, A.J. Ragauskas, Increasing the Carbohydrate  
614 Output of Bamboo Using a Combinatorial Pretreatment, ACS Sustain. Chem.  
615 Eng. 8 (2020) 7380–7393.

616 [7] H. Wu, L. Gong, X. Zhang, F. He, Z. Li, Bifunctional porous  
617 polyethyleneimine-grafted lignin microspheres for efficient adsorption of 2 , 4-  
618 dichlorophenoxyacetic acid over a wide pH range and controlled release,  
619 Chem. Eng. J. 411 (2021) 128539.

620 [8] X. Shen, Y. Xin, H. Liu, B. Han, Product-oriented Direct Cleavage of  
621 Chemical Linkages in Lignin, ChemSusChem. 13 (2020) 4367–4381.

622 [9] L. Xu, J. Zhang, Q.J. Zong, L. Wang, T. Xu, J. Gong, Z.H. Liu, B.Z. Li, Y.J.  
623 Yuan, High-solid ethylenediamine pretreatment to fractionate new lignin  
624 streams from lignocellulosic biomass, *Chem. Eng. J.* 427 (2022).

625 [10] Z.-M. Zhao, S. Zhang, X. Meng, Y. Pu, Z.-H. Liu, W.K. Ledford, S.M.K. II,  
626 B.-Z. Li, A.J. Ragauskas, As featured in : bioconversion by an alkali  
627 sterilization strategy †, *Green Chem.* 23 (2021) 4697–4709.

628 [11] M. Naebe, Y. Zhang, Lignin: A review on structure, properties, and  
629 applications as a light-colored UV absorber, *ACS Sustain. Chem. Eng.* 9  
630 (2021) 1427–1442.

631 [12] D. He, Y. Wang, C.G. Yoo, Q.J. Chen, Q. Yang, The fractionation of woody  
632 biomass under mild conditions using bifunctional phenol-4-sulfonic acid as a  
633 catalyst and lignin solvent, *Green Chem.* 22 (2020) 5414–5422.

634 [13] L. Shuai, M.T. Amiri, Y.M. Questell-santiago, F. Héroguel, Y. Li, H. Kim, R.  
635 Meilan, C. Chapple, J. Ralph, J.S. Luterbacher, Formaldehyde stabilization  
636 facilitates lignin monomer production during biomass depolymerization,  
637 *Science.* 354 (2016) 329–333.

638 [14] J. Wen, S. Sun, T. Yuan, F. Xu, R. Sun, Structural Elucidation of Lignin  
639 Polymers of Eucalyptus Chips during Organosolv Pretreatment and Extended  
640 Delignification, *Agric.Food Chem.* 61 (2013) 11067–11075.

641 [15] M. Hassanpour, M. Abbasabadi, L. Moghaddam, F. Fuelbiol, *Bioresource  
642 Technology* Mild fractionation of sugarcane bagasse into fermentable sugars  
643 and  $\beta$  -O-4 linkage-rich lignin based on acid-catalysed crude glycerol  
644 pretreatment, *Bioresour. Technol.* 318 (2020) 124059.

645 [16] Y. Liu, N. Deak, Z. Wang, P.J. Deuss, K. Barta, H. Yu, L. Hameleers, E. Jurak,  
646 Tunable and functional deep eutectic solvents for lignocellulose valorization,

647 Nat. Commun. 12 (2021) 1–15.

648 [17] Y.T. Tan, G.C. Ngoh, A. Seak, M. Chua, Bioresource Technology Effect of  
649 functional groups in acid constituent of deep eutectic solvent for extraction of  
650 reactive lignin, Bioresour. Technol. 281 (2019) 359–366.

651 [18] C. Huang, Y. Zhan, J. Cheng, J. Wang, X. Meng, X. Zhou, G. Fang, A.J.  
652 Ragauskas, Bioresource Technology Facilitating enzymatic hydrolysis with a  
653 novel guaiacol-based deep eutectic solvent pretreatment, Bioresour. Technol.  
654 326 (2021) 124696.

655 [19] W. Xing, G. Xu, J. Dong, R. Han, Y. Ni, Novel dihydrogen-bonding deep  
656 eutectic solvents : Pretreatment of rice straw for butanol fermentation featuring  
657 enzyme recycling and high solvent yield, 333 (2018) 712–720.

658 [20] Q. Xia, Y. Liu, J. Meng, W. Cheng, W. Chen, S. Liu, Y. Liu, J. Li, H. Yu,  
659 Multiple hydrogen bond coordination in three-constituent deep eutectic  
660 solvents enhances lignin fractionation from biomass, Green Chem. 20 (2018)  
661 2711–2721.

662 [21] S. Hong, X.J. Shen, Z. Xue, Z. Sun, T.Q. Yuan, Structure-function  
663 relationships of deep eutectic solvents for lignin extraction and chemical  
664 transformation, Green Chem. 22 (2020) 7219–7232.

665 [22] Z. Chen, X. Bai, H. Zhang, C. Wan, Insights into Structural Changes of Lignin  
666 toward Tailored Properties during Deep Eutectic Solvent Pretreatment, ACS  
667 Sustain. Chem. Eng. 8 (2020) 9783–9793.

668 [23] X. Shen, J. Wen, Q. Mei, X. Chen, D. Sun, T. Yuan, R. Sun, Facile  
669 fractionation of lignocelluloses by biomass-derived deep eutectic solvent  
670 (DES) pretreatment for cellulose enzymatic hydrolysis and lignin valorization,  
671 Green Chem. 21 (2019) 275–283.

672 [24] Z.K. Wang, S. Hong, J. long Wen, C.Y. Ma, L. Tang, H. Jiang, J.J. Chen, S. Li,  
673 X.J. Shen, T.Q. Yuan, Lewis Acid-Facilitated Deep Eutectic Solvent (DES)  
674 Pretreatment for Producing High-Purity and Antioxidative Lignin, ACS  
675 Sustain. Chem. Eng. 8 (2020) 1050–1057.

676 [25] A. Sluiter, B. Hames, R. Ruiz, C. Scarlata, J. Sluiter, D. Templeton, D.  
677 Crocker, Determination of structural carbohydrates and lignin in Biomass -  
678 NREL/TP-510-42618, Lab. Anal. Proced. (2012) 17.

679 [26] Z. Ling, Z. Guo, C. Huang, L. Yao, F. Xu, Bioresource Technology  
680 Deconstruction of oriented crystalline cellulose by novel levulinic acid based  
681 deep eutectic solvents pretreatment for improved enzymatic accessibility,  
682 Bioresour. Technol. 305 (2020) 123025.

683 [27] J.A. Sirviö, K. Hyypio, S. Asaadi, K. Junka, H. Liimatainen, High-strength  
684 cellulose nanofibers produced: Via swelling pretreatment based on a choline  
685 chloride-imidazole deep eutectic solvent, Green Chem. 22 (2020) 1763–1775.

686 [28] K.H. Kim, T. Dutta, J. Sun, B. Simmons, S. Singh, Biomass pretreatment using  
687 deep eutectic solvents from lignin derived phenols, Green Chem. 20 (2018)  
688 809–815.

689 [29] Z. Chen, W.D. Reznicek, C. Wan, Aqueous Choline Chloride: A Novel Solvent  
690 for Switchgrass Fractionation and Subsequent Hemicellulose Conversion into  
691 Furfural, ACS Sustain. Chem. Eng. 6 (2018) 6910–6919.

692 [30] L. Yang, Y. Ru, S. Xu, T. Liu, L. Tan, Bioresource Technology Features  
693 correlated to improved enzymatic digestibility of corn stover subjected to  
694 alkaline hydrogen peroxide pretreatment, Bioresour. Technol. 325 (2021)  
695 124688.

696 [31] C. Dong, X. Meng, C.S. Yeung, H.Y. Tse, A.J. Ragauskas, S.Y. Leu, Diol

697 pretreatment to fractionate a reactive lignin in lignocellulosic biomass  
698 biorefineries, *Green Chem.* 21 (2019) 2788–2800.

699 [32] Q. Chu, R. Wang, W. Tong, Y. Jin, J. Hu, K. Song, Improving Enzymatic  
700 Saccharification and Ethanol Production from Hardwood by Deacetylation and  
701 Steam Pretreatment: Insight into Mitigating Lignin Inhibition, *ACS Sustain.*  
702 *Chem. Eng.* 8 (2020) 17967–17978.

703 [33] T.R. Mota, D.M. Oliveira, R. Simister, C. Whitehead, A. Lanot, D. Wanderley,  
704 C.A. Rezende, S.J. Mcqueen-, L.D. Gomez, Bioresource Technology Design of  
705 experiments driven optimization of alkaline pretreatment and saccharification  
706 for sugarcane bagasse, *Bioresour. Technol.* 321 (2021) 124499.

707 [34] D. He, Y. Wang, C.G. Yoo, Q.-J. Chen, Q. Yang, The fractionation of woody  
708 biomass under mild conditions using bifunctional phenol-4-sulfonic acid as a  
709 catalyst and lignin solvent, *Green Chem.* 22 (2020) 5414–5422.

710 [35] C.S. Lancefield, I. Panovic, P.J. Deuss, K. Barta, N.J. Westwood, Pre-treatment  
711 of lignocellulosic feedstocks using biorenewable alcohols: Towards complete  
712 biomass valorisation, *Green Chem.* 19 (2017) 202–214.

713 [36] F.H.B. Sosa, D.O. Abranchedes, A.M. Da Costa Lopes, J.A.P. Coutinho, M.C. Da  
714 Costa, Kraft Lignin Solubility and Its Chemical Modification in Deep Eutectic  
715 Solvents, *ACS Sustain. Chem. Eng.* 8 (2020) 18577–18589.

716 [37] B. Soares, C. Lopes, A.J.D. Silvestre, P.C. Rodrigues, C.S.R. Freire, A.P.  
717 Coutinho, Industrial Crops & Products Wood delignification with aqueous  
718 solutions of deep eutectic solvents, *Ind. Crop. Prod.* 160 (2021) 113128.

719 [38] L. Wang, L. Xu, J. Zhang, Q. Zong, L. Wang, T. Xu, J. Gong, High-solid  
720 Ethylenediamine Pretreatment to Fractionate New Lignin Streams from  
721 Lignocellulosic Biomass High-solid ethylenediamine pretreatment to

722 fractionate new lignin streams from lignocellulosic biomass, *Chem. Eng. J.* 427  
723 (2021).

724 [39] X. Shen, T. Chen, H. Wang, Q. Mei, F. Yue, S. Sun, Structural and  
725 Morphological Transformations of Lignin Macromolecules during Bio-Based  
726 Deep Eutectic Solvent (DES) Pretreatment, *ACS Sustain. Chem. Eng.* 8 (2020)  
727 2130–2137.

728 [40] J.D. Zwilling, X. Jiang, F. Zambrano, R.A. Venditti, H. Jameel, O.D. Velev,  
729 O.J. Rojas, R. Gonzalez, Understanding lignin micro- And nanoparticle  
730 nucleation and growth in aqueous suspensions by solvent fractionation, *Green*  
731 *Chem.* 23 (2021) 1001–1012.

732 [41] J.L. Wen, S.L. Sun, T.Q. Yuan, R.C. Sun, Structural elucidation of whole  
733 lignin from Eucalyptus based on preswelling and enzymatic hydrolysis, *Green*  
734 *Chem.* 17 (2015) 1589–1596.

735 [42] J. Wen, B. Xue, F. Xu, R. Sun, A. Pinkert, Unmasking the structural features  
736 and property of lignin from bamboo, *Ind. Crop. Prod.* 42 (2013) 332–343.

737 [43] W. Lan, M.T. Amiri, C.M. Hunston, J.S. Luterbacher, Protection Group Effects  
738 During a , g -Diol Lignin Stabilization Promote High-Selectivity Monomer  
739 Production *Angewandte, Angew.Chem. Int.Ed.* 57 (2018) 1356–1360.

740 [44] C. Cai, K. Hirth, R. Gleisner, H. Lou, X. Qiu, J.Y. Zhu, Maleic acid as a  
741 dicarboxylic acid hydrotrope for sustainable fractionation of wood at  
742 atmospheric pressure and  $\leq 100$  °C: mode and utility of lignin esterification,  
743 *Green Chem.* 22 (2020) 1605–1617.

744 [45] Y. Liang, W. Duan, X. An, Y. Qiao, Y. Tian, H. Zhou, *Bioresource*  
745 *Technology* Novel betaine-amino acid based natural deep eutectic solvents for  
746 enhancing the enzymatic hydrolysis of corncob, *Bioresour. Technol.* 310

747 (2020) 123389.

748 [46] A. Romaní, E.S. Morais, P.O. Soares, M.G. Freire, C.S.R. Freire, A.J.D. Silvestre, L. Domingues, *Bioresource Technology* Aqueous solutions of deep eutectic systems as reaction media for the saccharification and fermentation of hardwood xylan into xylitol, *Bioresour. Technol.* 311 (2020) 123524.

752 [47] Y. Wang, X. Meng, K. Jeong, S. Li, G. Leem, K.H. Kim, Y. Pu, A.J. Ragauskas, C.G. Yoo, Investigation of a Lignin-Based Deep Eutectic Solvent Using p -Hydroxybenzoic Acid for Efficient Woody Biomass Conversion, *ACS Sustain. Chem. Eng.* 8 (2020) 12542–12553.

756 [48] L. Bui, H. Luo, W.R. Gunther, Y. Román-Leshkov, Domino Reaction Catalyzed by Zeolites with Brønsted and Lewis Acid Sites for the Production of  $\gamma$ -Valerolactone from Furfural, *Angew. Chemie.* 125 (2013) 8180–8183.

759 [49] T.M. Aida, Y. Sato, M. Watanabe, K. Tajima, T. Nonaka, H. Hattori, K. Arai, Dehydration of d-glucose in high temperature water at pressures up to 80 MPa, *J. Supercrit. Fluids.* 40 (2007) 381–388.

762 [50] M. Spangsberg, S. Shunmugavel, E. Taarning, Conversion of Sugars to Lactic Acid Derivatives Using Heterogeneous Zeotype Catalysts, *Science.* 328 (2010).